Conductance and Vibrational States of Single-Molecule Junctions Controlled by Mechanical Stretching and Material Variation

Youngsang Kim,[1,*] Hyunwook Song,[2,†] Florian Strigl,[1] Hans-Fridtjof Pernau,[1,‡] Takhee Lee,[2] and Elke Scheer[1,§]

[1]*Department of Physics, University of Konstanz, 78457 Konstanz, Germany*

[2]*School of Materials Science and Engineering and Department of Nanobio Materials and Electronics, Gwangju Institute of Science and Technology, Gwangju 500-712, Korea*

(Received 5 August 2010; published 13 May 2011)

The changes of molecular conformation, contact geometry, and metal-molecule bonding are revealed by inelastic-electron-tunneling spectroscopy measurements characterizing the molecular vibrational modes and the metal-phonon modes in alkanedithiol molecular junctions at low temperature. Combining inelastic-electron-tunneling spectroscopy with mechanical control and electrode material variation (Au or Pt) enables separating the influence of contact geometry and of molecular conformation. The mechanical strain of different electrode materials can be imposed onto the molecule, opening a new route for controlling the charge transport through individual molecules.

DOI: 10.1103/PhysRevLett.106.196804 PACS numbers: 73.63.Rt, 61.46.−w, 81.07.Nb

Extensive studies on charge transport through single molecules (SMs) have been performed for the implementation of molecular-scale devices and for understanding the charge transport mechanisms in such devices [1,2]. The conductance of the same SM contacted with a mechanically controllable break junction (MCBJ) or with a scanning tunneling microscope is reported to have various values because the contact geometry (CG) and the molecular conformation (MC) may vary [3,4]. To understand precisely such dependences, more sophisticated experimental studies are required [5]. The CG and the material of electrodes significantly influence the charge transport through the SM, although it is specifically anchored by functional end groups [6–9]. Alkanedithiol, having a simple and flexible structure, is one of the most appropriate candidates to study these properties and can adopt the usual *trans* (*T*) conformation as well as a *gauche* (*G*, or defect) conformation, which is predicted to give rise to alterations of the charge tunneling [3,10–12]. Inelastic-electron-tunneling spectroscopy (IETS) is very suitable for detecting vibrational excitations and is sensitive to CG and MC [2,12,13].

Here we discuss IETS measurements for 1,6-hexanedithiol [HS-$(CH_2)_6$-SH, denoted as HDT] molecules when stretching both Au and Pt MCBJs used as adjustable electrodes at low temperature. The signatures of the different MCs and CGs are demonstrated by the appearance of particular IETS signals as well as by changes in the conductance. This combined study provides a better understanding of charge transport in molecular junctions (MJs) by reporting several new and significant findings, including how the MCs are adopted, by the markedly different behavior of the metal-sulfur vibrational mode under stretching and by the observation of the extremity mode of molecular vibration under stretching. All these findings were enabled by the development of the lithographically defined Pt MCBJ.

The HDT molecules are connected to the electrodes formed by the MCBJ technique as illustrated in Fig. 1(a). The details of the device fabrication [14] are described in the supplemental material [15]. In order to determine the preferred conductance values of the MJs, we repeatedly opened and closed the junctions and recorded the conductance histograms as shown in Fig. 1(b). The inset in Fig. 1(b) presents typical conductance traces acquired during opening processes. In both histograms, two clear conductance maxima are observed and denoted as ''highest conductance'' (HC) and ''lowest conductance'' (LC), respectively, as indicated by the arrows. For the Au-HDT-Au we observe two additional intermediate conductance peaks. We assume that these peaks arise from multiple possible CGs of Au junctions. They have been observed and described theoretically previously [3]. We concentrate with our IETS measurements on the HC and LC regimes to analyze distinct changes and differences between the two electrode materials. The conductance values of these maxima are approximately twofold higher in the Pt-HDT-Pt junctions than for the Au-HDT-Au junctions, in agreement with previous studies [6]. The local density of states of the *d* band for Pt at the Fermi level (E_F) is higher by 1 order of magnitude than that of Au, resulting in an enhancement of the conductance [6–8,16]. The current-voltage (*I*-*V*) characteristics (see [15]) can be well described by the single-level model [17] for symmetric metal-molecule coupling for both junction types. No temperature dependence is observed, signaling that tunneling is the conduction mechanism.

Representative symmetric IETS spectra are shown in Fig. 1(c). The IETS spectra defined as $(d^2I/dV^2)/(dI/dV)$ are presented while separating the junction from the HC [Fig. 2(a)] to LC [Fig. 2(b)]. The distance scale is set to zero at the beginning of the HC plateau. After stretching the junction for 4.5 Å, the conductance jumps to the

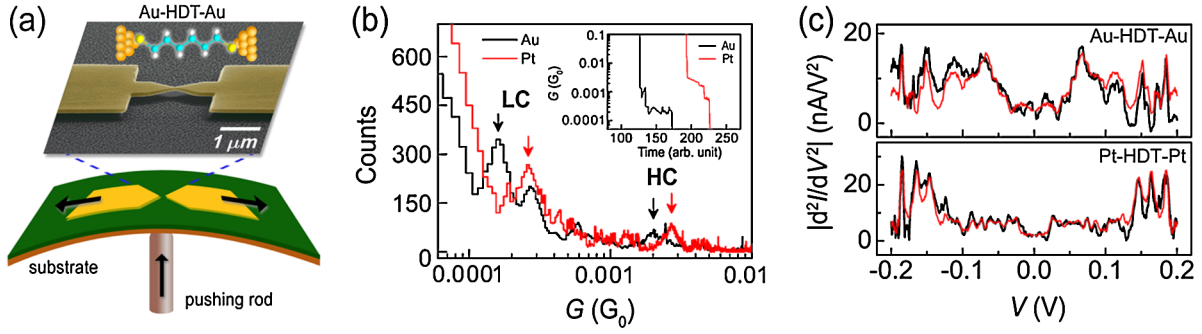

FIG. 1 (color online). (a) Schematic illustration of MCBJ system and scanning electron micrograph image of a sample with a scheme of a MJ. (b) Histograms of Au (black) and Pt (red) junctions, repeated 2000 and 300 times, respectively. Inset: Representative conductance traces. (c) IETS (black) of HDT connected with Au and Pt. For negative polarity, the sign of d^2I/dV^2 has been inverted for better illustration. The red lines are obtained by the simple formula ($y = [f(x) - f(-x)]/2$) which applies for the symmetrization of point-symmetric functions.

LC regime. We continuously stretched the junction to a total elongation of 14 Å. By comparison with previously studied IETS measurements and theoretical calculations, the vibrational peaks in the spectra are assigned: Z, longitudinal metal phonon; I, Au-S stretching [ν(Au-S)]; II, C-S stretching [ν(C-S)]; III, C-H rocking [$\delta_r(CH_2)$]; IV, C-C stretching [ν(C-C)]; V, C-H wagging [$\gamma_w(CH_2)$]; VI, C-H scissoring [$\delta_s(CH_2)$] (see also [15], Table S1).

The shapes of IETS spectra in HC of Fig. 2(a) and LC of Fig. 2(b) vary, because the IETS depends on the MC, the atomic arrangement, and the metal-molecule coupling, influencing the conductance as well [3,18,19]. First, we investigated potential changes in MC, e.g., the T and G conformations for the Au-HDT-Au junctions. The T conformation is the usual one, in which the H atoms attached to neighboring C atoms are positioned opposite to each other. If one G defect is present, the H atoms attached to the two neighboring C atoms are rotated roughly 120°, and the C chain has a kink [see Fig. 2(d)]. In HDT with six carbons, several G defects may appear. In simulations, the appearance of only one G effect has been shown to be sufficient to adapt the molecule to a given electrode spacing [3,10]. As shall be explained below, we attribute the spectra shown in blue to the molecule being in the G conformation. The T conformation has been predicted to have higher conductance than the G conformation by roughly 1 order of magnitude [3,10,11,19]. The current-carrying molecular orbital is delocalized in the T conformation, whereas the overlap of the molecular orbitals is weaker in the G conformation [3,11,20]. We analyze the conductance values obtained just before the corresponding IETS measurements, as shown in Fig. 2(e). Sudden drops or increases of the conductance are taken as criterion for a conformational change from the T to the G conformation or vice versa and are used for color coding the spectra. In the inset in Fig. 2(e), the average conductance change between both conformations is found to be a factor of 3; however, for individual junctions it amounts to roughly a factor of 5, which is in reasonable agreement with theoretical expectations [10,11].

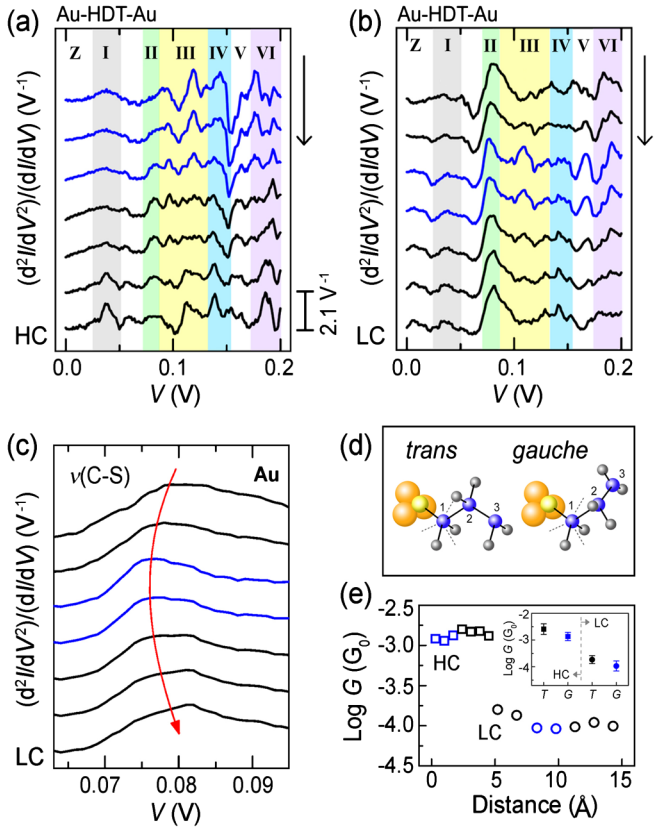

FIG. 2 (color online). (a),(b) IETS in the HC (a) and the LC (b) regimes, displaced vertically in the order of the junction distances in the Au-HDT-Au junction. The IETS are measured from a distance of 0.5 (top) to 4.5 Å (bottom) for the HC regime (a) and between 5 (top) and 14 Å (bottom) for the LC regime (b). The distance axis is set to zero when the conductance first dropped below 0.1 G_0. (c) Enlarged ν(C-S) mode reported in (b). (d) Schematic diagrams of both T and G conformations. (e) Conductance recorded just before the measurement of the IETS while increasing the electrode distances. Inset: Averages (over all junctions) with standard deviations of the conductance values in the T (black) and G (blue) conformations.

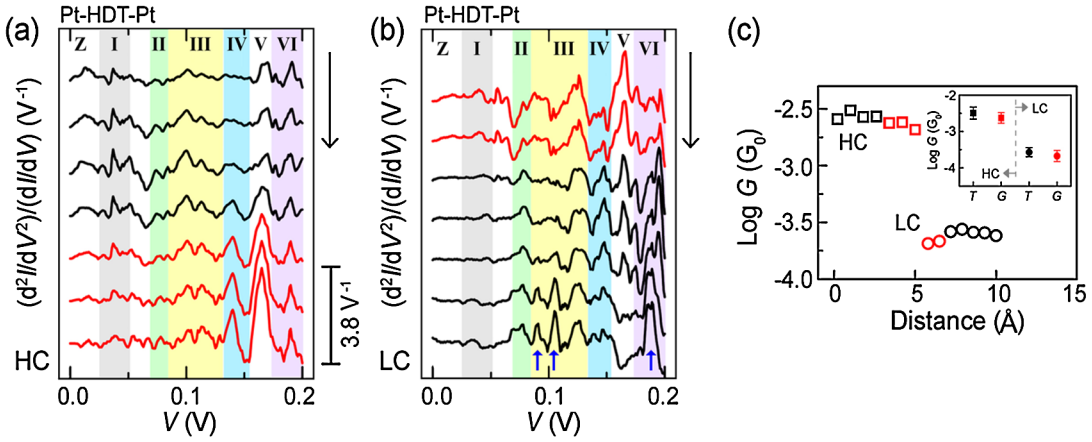

FIG. 3 (color online). (a), (b) IETS in the HC (a) and the LC (b) regimes in the Pt-HDT-Pt junction approximately between 0.2 (top) and 5 Å (bottom) for the HC regime (a) and between 6 (top) and 10 Å (bottom) for the LC regime (b). (c) Conductance values obtained just before the IETS measurement. Inset: Average conductance values in the T (black) and G (red) conformations.

This interpretation is strongly supported by the IETS measurements: the redshift of ν(C-S) and the enhanced intensity of $\delta_r(CH_2)$ and $\gamma_w(CH_2)$. The redshift of ν(C-S) can be caused by the reduction of the electron density at the C-S bonds, owing to the weaker overlap of the orbitals in the G conformation [3,10,21]. We observe a redshift of the ν(C-S) peak by ~4 mV, as shown in Fig. 2(c). The stronger intensity in $\delta_r(CH_2)$ and $\gamma_w(CH_2)$ is also consistent with the interpretation of the G defect, because in this conformation the C-H bonds become nearly perpendicular to the metal surface (parallel to the conduction path) and are thus easier to excite by the conduction electrons [10,21,22]. Those spectra indicate the G conformation. They are highlighted in blue in Figs. 2(a) and 2(b).

In the same manner, we carried out IETS measurements for Pt-HDT-Pt junctions. Figures 3(a) and 3(b) are measured in HC and LC regimes, respectively. The vibrational modes are the same as assigned in the Au-HDT-Au junction, except for the Pt-S stretching mode [ν(Pt-S)], indicating that the end group of HDT is connected robustly with the Pt [22]. The G conformation is shown in red in the IETS spectra and the conductance trace in Fig. 3(c).

To reveal the different CGs, we compared the total stretching distance. Analysis of our data shows a stretching distance of 15 and 10 Å for Au-HDT-Au and Pt-HDT-Pt junctions, respectively, and is in good agreement with previous experimental and theoretical studies [23,24]. The averaged stretching distances are demonstrated in [15]. These results indicate that the bonding strength of Au atoms is weaker than that of Pt atoms. This interpretation is strongly supported by the excitation of metal-phonon modes. We observed enhanced IETS peaks around 18 mV [the longitudinal Au phonon, Z mode in Figs. 2(a) and 2(b)] in Au-HDT-Au junctions as shown in Fig. 4(a). The inset in Fig. 4(a) shows the enhancement (due to the increase of electron-phonon interaction) and the redshift (due to the decrease of elastic constant) of the IETS peak under stretching, which indicate that the Au atoms form a chain in one dimension [25]. However, in Pt electrodes, we have not observed the enhancement of the Z mode of Pt [at 12 mV in Fig. 3(a) and 3(b)], indicating that the Pt atoms do not form long chains under stretching. To further reveal the influence of the CG, we study the variation of both ν(Au-S) and ν(Pt-S) as a function of junction distance as shown in Fig. 4(b). In the HC regime, the modes are stable, showing the same peak positions, whereas these change abruptly when the conductance jumps to the LC regime. Such discontinuous change in the metal-S stretching mode is caused by a motion of the end group along the metal atoms, like a hopping from one metal site to another. It was theoretically studied that the metal-S bonding energy and the conductance can change remarkably when the bonding site is altered upon stretching the MJs [4,26]. For the slight change of ν(Au-S) in the LC regime in Fig. 4(b), we assume that the Au-Au bonds (rather than the Au-S bonds) are elongated, forming long chains due to the weak bonding strength of Au atoms. However, in the case of Pt-HDT-Pt, we detected a pronounced variation (maximum $\Delta E \sim 12$ mV) of the energy of the ν(Pt-S) in the LC regime. These findings can be

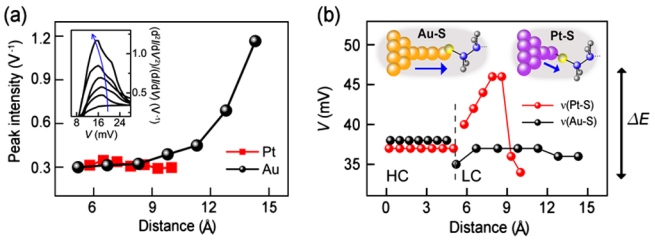

FIG. 4 (color online). (a) IETS intensity of the Z mode of Au (black) and Pt (red) [in Figs. 2(a), 2(b), 3(a), and 3(b)] while stretching. Inset: Enhancement and redshift of Au phonon spectra obtained from another set of IETS spectra. (b) Frequency shift for ν(Au-S) (black) and ν(Pt-S) (red) modes as a function of distance (extracted from the data set of Figs. 2 and 3).

interpreted as follows: When stretching a metal-molecule bond from the equilibrium position (energy minimum), the restoring force and thus the resonance frequency may behave analogously to the frequency increase when stretching a guitar string. When the stretching force exceeds the binding force, it is weakened, because at larger distances the overlap of the atomic orbitals forming the Pt-S bond is reduced [16,23]. This nonmonotonic development of a chemical bond upon stretching is at variance to the behavior of, e.g., vibrational modes of hydrogen under stretching [9]. It might be specific to the Pt-S bond, presumably because of the nonspherical *d*-electron wave functions of Pt. We show a conceptual image of this situation in the inset in Fig. 4(b). Especially in the Pt-HDT-Pt junctions, the strong additional peaks around 100 and 180 mV, indicated by blue arrows in the fully stretched regime in Fig. 3(b), are observed at a lower energy than the respective modes of the uncoupled molecule. We therefore interpret them as being the extremity modes of $\delta_r(CH_2)$ and $\delta_s(CH_2)$ [20]. When the Pt-S bonds become weakened by a further stretching of the junction, the adjacent CH_2 vibrations can be staggered and localized at the end of the molecular backbone, resulting in the appearance of an extremity mode of the CH_2 groups [21]. The scenario involving T/G conformational changes as well as chain formation of the Au electrodes under stretching coherently describes the totality of our experimental findings. Alternative schemes including changes of the tilt angle of the SM in the junction or varying adsorption site of the S atoms on the electrode metal are discussed in [15].

The systematic comparison study of the stretching dependence for IETS spectra of HDT single-molecule junctions with Au and Pt electrodes clearly shows different molecular conformations. By tracing the metal-sulfur vibrational modes under stretching, we have unambiguously demonstrated the impact of the electrode metal on both the molecular conformations and the contact geometry. With the rather stiff Pt as adjustable nanoelectrodes, instead of the conventional and smooth Au, we have been able to excite and to tune particular vibrational modes, e.g., the extremity modes of a molecule. Such new combination of methodologies will pave the way to establishing a detailed correlation between the precise atomic arrangement and the conductance properties of molecular junctions.

We thank T. Frederiksen, W. Wulfhekel, J. M. van Ruitenbeek, and A. Erbe for fruitful discussions. This work was supported by the DFG through SFB767 and the Krupp Foundation. H. S. and T. L. thank the National Research Laboratory and World Class University programs from Korea.

*youngsang.kim@uni-konstanz.de
†Present address: Department of Electrical Engineering and Applied Physics, Yale University, New Haven, CT 06520, USA.
‡Present address: Fraunhofer-Institute for Physical Measurement Techniques, Thermoelectric Systems, 79110 Freiburg, Germany.
§elke.scheer@uni-konstanz.de

[1] M. Galperin *et al.*, Science **319**, 1056 (2008); M. A. Reed *et al.*, Science **278**, 252 (1997); H. Song *et al.*, Nature (London) **462**, 1039 (2009).
[2] J. G. Kushmerick *et al.*, Nano Lett. **4**, 639 (2004); W. Wang *et al.*, Nano Lett. **4**, 643 (2004); L. H. Yu, C. D. Zangmeister, and J. G. Kushmerick, Phys. Rev. Lett. **98**, 206803 (2007).
[3] C. Li *et al.*, J. Am. Chem. Soc. **130**, 318 (2008).
[4] M. Kamenetska *et al.*, Phys. Rev. Lett. **102**, 126803 (2009).
[5] J. J. Parks *et al.*, Phys. Rev. Lett. **99**, 026601 (2007).
[6] C.-H. Ko *et al.*, J. Am. Chem. Soc. **132**, 756 (2010); V. B. Engelkes, J. M. Beebe, and C. D. Frisbie, J. Am. Chem. Soc. **126**, 14 287 (2004).
[7] J. W. Lawson and C. W. Bauschlicher, Jr., Phys. Rev. B **74**, 125401 (2006).
[8] J. M. Seminario, C. E. De La Cruz, and P. A. Derosa, J. Am. Chem. Soc. **123**, 5616 (2001).
[9] D. Djukic *et al.*, Phys. Rev. B **71**, 161402 (2005).
[10] M. Paulsson *et al.*, Nano Lett. **9**, 117 (2009).
[11] D. R. Jones and A. Troisi, J. Phys. Chem. C **111**, 14 567 (2007).
[12] C. R. Arroyo *et al.*, Phys. Rev. B **81**, 075405 (2010).
[13] M. Paulsson *et al.*, Phys. Rev. Lett. **100**, 226604 (2008).
[14] T. Böhler, A. Edtbauer, and E. Scheer, Phys. Rev. B **76**, 125432 (2007).
[15] See supplemental material at http://link.aps.org/supplemental/10.1103/PhysRevLett.106.196804 for a detailed explanation.
[16] M. Kiguchi *et al.*, Appl. Phys. Lett. **91**, 053110 (2007).
[17] L. A. Zotti *et al.*, Small **6**, 1529 (2010).
[18] A. Troisi and M. A. Ratner, Nano Lett. **6**, 1784 (2006).
[19] D. A. Luzhbin and C.-C. Kaun, Phys. Rev. B **81**, 035424 (2010).
[20] C. B. George, M. A. Ratner, and J. B. Lambert, J. Phys. Chem. A **113**, 3876 (2009).
[21] G. C. Solomon *et al.*, J. Chem. Phys. **124**, 094704 (2006).
[22] A. Kudelski, Vib. Spectrosc. **39**, 200 (2005).
[23] R. H. M. Smit *et al.*, Phys. Rev. Lett. **87**, 266102 (2001).
[24] F. Pauly *et al.*, Phys. Rev. B **74**, 235106 (2006).
[25] N. Agraït *et al.*, Phys. Rev. Lett. **88**, 216803 (2002).
[26] R. Zhang *et al.*, Nanotechnology **21**, 155203 (2010).